Soft Matter

Dynamic Article Links

Cite this: *Soft Matter*, 2012, **8**, 4740

www.rsc.org/softmatter

PAPER

Influence of adsorbed polyelectrolytes on pore size distribution of a water-swollen biomaterial†

Niko Aarne, Eero Kontturi* and Janne Laine

Received 30th November 2011, Accepted 26th January 2012
DOI: 10.1039/c2sm07268h

Many biomaterials exhibit pronounced swelling and consequently pronounced porous structure when exposed to water. Characterization and tuning of the porosity are important for the fundamental understanding of the behaviour of the biomaterials as well as for many of their applications, both traditional and novel. Here, the porous structure of cellulosic fibres (chemical wood pulp) was analysed in the wet state by differential scanning calorimetry (DSC) with and without adsorbed cationic polyelectrolytes. The polyelectrolytes were low molecular weight (M_w) high charge polybrene (hexadimethrine bromide) and two high M_w high charge PDADMACs (poly(diallyldimethyl ammonium chlorides)) with well-defined M_w distributions. The porosity changes upon adsorption of cationic polyelectrolytes in the wet-state were followed and the pore analysis gave insights into the distribution of the pores in the wet-state and into the changes of the porous structure in the surface as well as within the whole cell wall. By utilizing the well characterized polyelectrolytes we were able to detect subtle changes in the micropores of cellulosic fibres due to the adsorbed polyelectrolytes. The polymers did not affect the pore volumes in the 2.5–17 nm region upon drying, an important finding considering the porosity. Overall, the cationic polyelectrolytes decreased the pore volume by reducing the osmotic pressure. In addition, the results were compared to a physical state change, *i.e.*, drying and rewetting, to observe and compare the wetting hysteresis of the aforementioned fibres.

Introduction

Much is known about polyelectrolyte adsorption on porous substrates, both for static pores and for the kind of pores whose existence depends on swelling of the material in an aqueous environment.[1–3] In addition, the exceptional behaviour of polymers inside small pores has been elaborated.[4] However, little is known about the influence of adsorbed polyelectrolytes on the pore size distribution of water-swollen materials. In this paper, the issue of pore size in a common bio-based material, namely cellulosic fibres, upon adsorption of various cationic polyelectrolytes has been addressed.

Native cellulosic fibres are biomaterials swollen by water.[5,6] They consist of semi-crystalline agglomerates of cellulose chains called cellulose microfibrils whose length runs up to several micrometres and width ranges from 2–20 nm. Microfibrils do not fill the space completely in the fibre cell wall and the space between the microfibrils is partially filled by water in an aqueous environment, resulting in the formation of pores with diameters from 1 nm onwards (Fig. 1).[7] However, if the wet structure is dried, virtually all the (<1 μm) pores close, some of them irreversibly. In the water swollen state, the pore size of fibres is not dictated by covalent cross-linking—as in conventional hydrogels—but it is largely determined by the geometrical constraints of the hierarchically structured plant cell wall (Fig. 1). Other factors affecting the pore size include the chemical composition of the fibres, the degree of crystallinity in cellulose microfibrils, and the fibre charge. The crystallinity of cellulose in wood-based, chemical pulp fibres generally varies between 50% and 70%.[8]

Porosity of cellulosic fibres is vastly important in practical applications such as papermaking or textile manufacturing and it has, therefore, received a lot of coverage in applied research.[11–13] Polyelectrolyte adsorption onto fibres has also been subject to extensive research, mainly from the technical perspective in papermaking.[14–16] On the other hand, the usage of paper-based materials has recently expanded to sophisticated analytical platforms,[17,18] catalyst carriers,[19] magnetic nanocomposites,[20] and patterned templates for reactant delivery[21] among others. Particularly in the light of these novel applications, the pore size of water-swollen cellulosic materials and its tuning *via* simple routes like polyelectrolyte adsorption are relevant issues. Occasionally, the effect of pores within the fibres has been specifically addressed from the point of view of polyelectrolyte adsorption but, to our knowledge, never *vice versa*, and the studies have been

Department of Forest Products Technology, School of Chemical Technology, Aalto University, P.O.Box 16300, 00076 Aalto, Finland. E-mail: eero.kontturi@aalto.fi; Fax: +358 947024259; Tel: +358 94702450

† Electronic supplementary information (ESI) available. See DOI: 10.1039/c2sm07268h

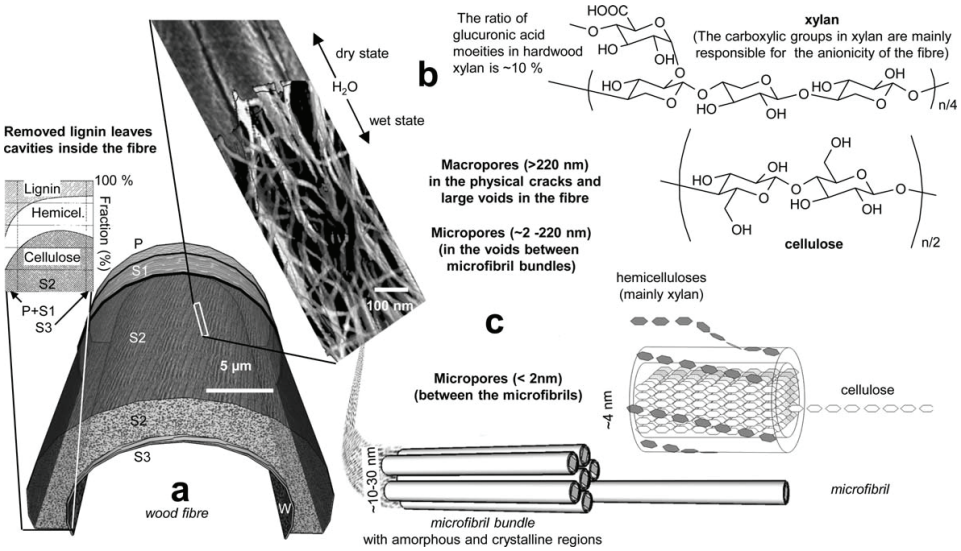

Fig. 1 A schematic representation of the fibre, the primary constituents of wood fibre, the morphological changes induced by drying and the location of the pores. (a) A schematic representation of a wood fibre. The fibre is composed of primary wall (P), secondary wall (S1, S2 and S3) and the warty layer (W). The composition of the fibre changes during delignification processes (pulping and bleaching); lignin is almost totally removed and some hemicellulose losses can be expected along with some damage to P, S1 and W layers. The delignification process also yields pores of various sizes and they are mainly located in the thickest layer S2. (b) Two different morphological states of the fibre are represented in the schematic magnification. Introducing water to the fibre structure swells the fibre which generates a porous structure (wet state). Water removal closes the porous structure and some of the pores are irreversibly closed (dry state). (c) The micropores (~2 to 220 nm) are shown in the magnification of the surface and they can extend inside the wall, and if defibration has occurred (*e.g.* during refining), also in a gel phase near the surface. Larger pores (>220 nm) can be found in the physical cracks and large voids in the fibre. The micropores (<2 nm) are generally been accepted to be located in the cavities formed by the amorphous hemicelluloses.[9] Approximate amounts of different components of the cell wall were adapted from the work of Panshin *et al.*[10]

usually technical in nature.[1] Since the adsorbed polyelectrolytes affect the charge of fibres, it is logical to expect that the osmotic pressure towards the pores is consequently influenced. Adsorbed polyelectrolytes also possess a physical volume which can alter the size of the smallest pores. This work is a fundamental effort to explore the actual influence of adsorbed polyelectrolytes on the pore size distribution of chemical pulp fibres. Therefore, we have employed cationic polyelectrolytes of high and low molecular weight. Chemical pulp fibres and once-dried chemical pulp fibres were applied as substrates in order to investigate the effect of different pore size distributions between materials with similar chemical compositions. Chemical pulp is a particularly suitable substrate for this work since wood-based cellulosic fibres possess a grossly increased aqueous porosity after chemical pulping has been applied to remove non-carbohydrate components—namely lignin—from between the microfibrils. The actual wet-state porosity is still under debate with pore size diameters ranging from 2–2000 nm (typically in the order of 20 nm) depending on the analytical method of choice.[22–25] A bimodal distribution is also possible (Fig. 1). We used thermoporosimetry (TPM) with a differential scanning calorimeter (DSC) to probe the pore size distribution of the fibres in the swollen state. It is a method that has gained increasing interest when studying the effects of water swollen materials.[26–30] TPM is based on the triple-point shift of melting of frozen water inside the cavities, which is summarized by the Gibbs–Thomson equation.[31]

Experimental part

Materials

The pulp fibres were obtained from fully bleached (elementary chlorine free bleaching) chemical pulp produced in Botnia, Äänekoski, Finland. The kappa number of the pulp, reflecting its minute lignin content, was ~1 and the intrinsic viscosity 890 cm^3 g^{-1}, corresponding to a degree of polymerization of 4700 ($DP = ((1.65[\eta] - 116[\text{hemi}])\cdot[\text{cellulose}]^{-1})^{1.111}$) (ref. 32) for the cellulose in fibres. The carbohydrate composition of the fibres is reported in Table 1. These values correlate well with previous literature values of bleached hardwood kraft pulp fibres.[33] To obtain plain fibres, the fines were removed from the pulp through 200 mesh with 6.0 g dm^{-3} consistency, mixing and 5.0 dm^{-3} min^{-1} tap water (conductivity 200 μS cm^{-1}) for 1 h 30 min to give a clear filtrate

Table 1 Characterization of the cellulosic biomaterial

Sugars analyzed	mg/100 mg
D-(+)-Glucose	70.8
D-(+)-Xylose	28.6
D-(+)-Mannose	0.6
L-Rhamnose	<0.1
D-(+)-Galactose	<0.1
Total	100.0

(adapted from SCAN-M 6:69 standard). The counterions of the carboxylic groups in the fibres were converted into protons by first washing them with deionized water, then stirring the mixture for 60 min in 0.010 M HCl solution and finally washing it with deionized water twice to obtain a conductivity of 3.2 μS cm^{-1}. The protonated counterions were then converted to sodium ions by using 0.005 M $NaHCO_3$ and adjusting the pH to 8 by 1 M NaOH. This solution was mixed for 40 minutes and washed with deionized water until the conductivity was 3.1 μS cm^{-1}. This is a standard procedure for ensuring that all carboxylic groups in fibres have the same counterion (Na^+).[1,34] The polyelectrolytes were hexadimethrine bromide (polybrene, [3,6]-ionene, ≥94%, Sigma-Aldrich), two poly(dimethyldiallyl ammonium chloride) (PDADMAC, Sigma-Aldrich 400 000–500 000 g mol^{-1} and Salcare SC30 Ciba Specialty chemicals Ltd, Low Moor, Bradford, England, ultrafiltered within an Amicon ultrafiltration unit with a cut off of >300 000 g mol^{-1}), and sodium polyethylenesulfonate (PES-Na, M_w 19 100 g mol^{-1} Oy G. W. Berg & CO Ab/BTG Mütek GmbH). Other reagents were water (conductivity 0.5 μS cm^{-1}), 1 M hydrochloric acid solution (HCl, Merck Titripac), 1 M sodium hydroxide solution (NaOH, Merck Titripac), sodium hydrogen carbonate ($NaHCO_3$, GPR Rectapur (100%), VWR), and sodium chloride (NaCl, Merck). Molecular weight distributions were analyzed by size exclusion chromatography (SEC, Table 2). For cationic polyelectrolytes the measurement conditions were as follows: Agilent 1100 (Agilent, USA) with a refractive index detector, conventional calibration standard, and polyethyleneoxide with M_w 1.9 × 10^3 to 1.3 × 10^6 g mol^{-1}. The column was TSK $GMPW_{XL}$ (Tosoh, Japan). Measurement parameters were, flow: 0.5 cm^3 min^{-1}, mobile phase: 0.3125 mol dm^{-3} CH_3COOH and 0.3125 mol dm^{-3} CH_3COONa, at 35 °C.

Adsorption of cationic polyelectrolytes

Adsorption was performed in 6.0 g dm^{-3} pulp consistency with the polyelectrolyte concentration ranging from 0 to 0.12 g dm^{-3} in 1 mM $NaHCO_3$ solution (pH 8.2 ± 0.2) for 30 min under magnetic stirring. 30 minutes was regarded as a sufficient time for the adsorption to occur to the full extent based on earlier accounts.[35] The fibres were washed with deionized water in a dynamic drainage analyzer (DDA, Akribi Kemikonsulter Ab, Sundsvall, Sweden) directly afterwards. The dynamic drainage analyzer consists of a plastic vessel (~1 dm^3 volume) with a 10 cm diameter 100 mesh at the bottom. −0.25 bar vacuum is used to increase dewatering. The adsorption of cationic polyelectrolytes was determined from the filtrate by a MÜTEK particle charge detector (PCD-03, Mütek Analytic, Herrsching, Germany). The filtrate was titrated by 0.0020 N (2.0 meq dm^{-3}) PES-Na solution to the endpoint where streaming potential changed sign. Titrant consumption of the anionic polyelectrolyte solution and adsorbed pulp filtrate was equated to the charge density of the cationic polyelectrolyte. The after/before meq-ratio was used to calculate the adsorbed amount on the fibres. Charge determinations were made at pH 8.2 ± 0.2 in 1 mM $NaHCO_3$.[36]

Table 2 Properties of the polymers used. M_w and polydispersity index (PDI) measured by SEC, charge density (CD) according to specifications. Hydrodynamic diameter (D_h) measured with dynamic light scattering in 0.1 M NaCl

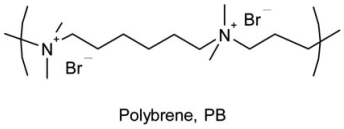

Polybrene, PB

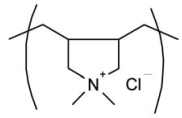

PDADMAC

	M_w/Da	PDI	CD/meq g^{-1}	D_h/nm
Polybrene, PB	6.3 × 10^3	1.8	5.34	3.0
PDADMAC, fractionated	3.2 × 10^5	3.2	6.19	41
PDADMAC, unfractionated	1.1 × 10^6	27	6.19	78

Pulp drying

DDA was used to obtain sheets with grammage 600 ± 30 g m^{-2}. These 10 cm diameter round sheets were clamped with a screw press between heavy rings of aluminium with 10 cm diameter, with sufficient pressure applied to the 0.3 cm thick rim. Sheets were dried with geometrical restriction at 80 °C for 60 min to gain a dry-matter content of 95 ± 1%. The pressed area was cut and the remaining sheet was rewetted overnight and disintegrated.

Water retention value (WRV) measurements

WRV measurements of fibres in their Na^+ form were done with a GR 4.22 centrifuge (Jouan, Saint-Herblain, France) according to SCAN-C 62:00 with slight modification. Deionized water was applied instead of the 0.0083 M (1 g dm^{-3}) $MgSO_4$. Error of the measurements, according to standard, are in the order of ~2%.

Thermoporosimetry (TPM) measurements

The measurement is based on the decrease in the melting point of a liquid confined in small pores. We used the Gibbs–Thomson equation, modified for fibrous material by Maloney:[31]

$$d = \frac{4VT_0\sigma_{ls}}{H_m\Delta T} = \frac{k}{\Delta T}$$

where V is the molar volume, σ_{ls} is the interfacial tension between solid (ice) and liquid (water), T_0 is the melting point at NTP, H_m is the latent heat of melting, and the constant $k = 43.12$ nm K for cylindrical pores with diameter d. Other derivations for k are found in the literature.[26,37] We applied this method because it has been adjusted with Hg porosimetry[31] and extensively calibrated with a series of controlled pore glasses (CPGs) and high purity silica gel samples, which also took the thermal electromotive force (EMF) distortions into account.[27] The isothermal step melting method was chosen because of its suitability for soft biomaterials with relatively large pores, such as pulp fibres.[27] In addition, the cryoscopic effect to the melting point is very minor in the applied ionic strength, namely in the order of 10^{-4} K (see Section S2 in the ESI† for calculations).

A Mettler-Toledo DSC 821 Differential Scanning Calorimeter with an intracooler and autosampler was used. Gas was N_2. Elaborate calibration was made to achieve ±0.02 °C accuracy in the region −50 to 0 °C.[27] Measurement points were −33 °C, −20 °C, −17 °C, −14 °C, −11 °C, −9 °C, −7 °C, −5 °C, −3.5 °C,

−2.5 °C, −1.6 °C, −0.8 °C, −0.4 °C, and −0.2 °C. Each temperature was retained for 7–10 minutes to ensure that all the water had melted before ramping to the next temperature. The ramping speed was 1.0 °C min^{-1}, which largely negates the thermo-EMF distortions which can cause additional error in the isothermal step melting procedure.[30] The moisture content of the samples varied between 1 and 2 g per g with most of the samples in the optimal region of 1.2–1.5 g per g. The pore volume for a given pore diameter was evaluated from the power-time area in each of the isothermal steps, and non-freezing water (NFW) was evaluated by melting and refreezing the sample and subtracting the total freezing water from the moisture content of the sample according to the method described by Maloney and Paulapuro.[31,38] ESI† is available for example data.

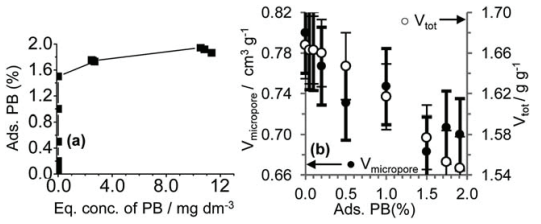

Fig. 2 (a) Adsorption isotherm of polybrene (PB), adsorption of PB plotted against the equilibrium concentration of PB. (b) The fibre cell wall water as measured by WRV (V_{tot}) and micropore water ($V_{micropore}$) including the NFW from thermoporosimetry (TPM), as a function of adsorbed PB.

Hydrodynamic diameter

To estimate the hydrodynamic diameter of the polyelectrolytes, a dynamic light scattering (DLS) device Malvern Zetasizer Nano ZS (Malvern Instruments, Malvern, U.K.) was used. The salt concentration was 0.1 M NaCl. Such a high concentration was chosen to suppress the electrostatic interaction between the segments of the polyelectrolytes and to collapse the structure in order to avoid the known difficulties of measuring non-spherical particles with DLS.

Results and discussion

General characteristics of the fibres

The substrate, bleached birch kraft pulp, is commonly applied in the pulp and paper industry and its physical and chemical properties have been extensively covered in the relevant literature. It is a porous, soft biomaterial consisting mainly of cellulose and xylan (a hemicellulose, see Fig. 1). The carbohydrate composition, as determined by HPLC (Table 1), reveals that the composition of the material used is similar to the ones published previously.[33] The sugar monomers consist mostly of glucose and xylose with a small amount of mannose, indicating that the polysaccharides in the pulp fibres are cellulose (constructed from anhydroglucose monomers) and xylan (constructed principally from xylose monomers). The charge of the fibre is mainly due to xylan, because the cellulose backbone lacks charged functional groups. In xylan, the specific nature of the compound responsible for the negative charge is altered when different bleaching methods are employed in the manufacturing processes of chemical pulp. Nevertheless, the main source of negative charge is due to the 4-*O*-methyl-D-glucuronic acid (GlcA), most of which has been transformed to 4-deoxy-β-L-threo-hex-4-enopyranosyluronic acid (HexA) in xylan during the processing from wood to pulp. According to the literature, these acid groups contribute approximately 10 mol% to the total amount in a xylan molecule (see Fig. 1),[39] which corresponds to the experimental total charge of the fibres as determined from a polyelectrolyte adsorption isotherm (Fig. 2a), *ca.* 80 μeq g^{-1}.

Cellulose resides in the fibre cell wall in semi-crystalline microfibrils whose orderly alignment is largely responsible for the hierarchical structure of the fibre (Fig. 1). The porosity is largely caused by the delignification processes routinely employed on this kind of biomaterial. The removal of lignin leaves voids between the cellulose microfibrils with xylan wrapped around the microfibrils and the voids are filled with water, resulting in a porous structure.[40] (The semicrystalline cellulose microfibrils themselves are largely impenetrable by water.) The amount of water in pores, *i.e.*, the extent of swelling, is largely influenced by the amorphous xylan whose dissociated carboxylic groups promote the swelling until the swelling is suspended by the hierarchical structure of the fibre cell wall (Fig. 1). The swelling of cellulose gel is caused by the hydration of hydroxyl groups in the cellulose as well as an osmotic pressure differential resulting from a difference in concentration of mobile ions between the interior of the gel and the exterior solution. The driving force, the source of osmotic pressure, is the presence of dissociated acidic groups in the fibre matrix.[41] Reversal of the swelling process, *i.e.*, deswelling, occurs when the electrostatic effect of these groups is neutralized by low pH, increased salt addition, or, in our case, the complexation and neutralization by cationic polyelectrolytes. The counter-ions play also an important role in how the adsorption occurs and how much water can be retained in the cell wall. Scallan and Grignon[42] argue that the free cations, which are not tightly bound to the carboxylate groups, cause swelling due to osmosis in the cell wall matrix. The osmotic effect is largest for the sodium ions and smaller for divalent or multivalent cations due to the close association of the multivalent cations with carboxylic groups. In our work we used sodium as the counter-ion to maximize the swelling of fibres and to control the ion-exchange phenomenon in polyelectrolyte adsorption.

The interplay between the swelling and deswelling effects together with geometrical constraints of the cell wall results in a so-called fibre saturation point which reflects the amount of water in the fibre cell wall. It can be measured indirectly by water retention value (WRV)—a method where excess water is removed from a fibre suspension by centrifugation and only the water responsible for the swelling inside the fibre cell wall can be quantified.[28,43] More information on swelling can be obtained by TPM that provides information on the actual pore size distribution within the swollen fibres. TPM is based on the depression of the melting point of frozen water within the capillaries. The melting point depression of a gradually heated frozen sample is step converted to the size of a cylinder with given diameter by the Gibbs–Thomson correlation.[31]

Adsorption *vs.* porosity with never-dried fibres

Low M_w high charge polyelectrolyte adsorption. Fig. 2a presents the adsorption isotherm of a small M_w polyelectrolyte polybrene on chemical pulp fibres. The plateau level, after which polybrene is no longer stoichiometrically adsorbed, is 1.5% (15 mg g^{-1}). As mentioned earlier, the cationic polyelectrolytes are bound to deswell the cellulosic fibres upon their adsorption. The deswelling behaviour is quantitatively demonstrated in Fig. 2b where WRV and pore volume (as measured by TPM) values are plotted as a function of the adsorbed polybrene. The pore volume correlates with the decrease in WRV when incremental amounts of polybrene are adsorbed onto the fibres. WRV and pore volume begin to settle at 1.55 and 0.69 g per g, respectively—there is a limit of how much deswelling adsorption can impose on a fibre. After this nominal value, the dissociated acidic groups of the fibre accessible to the cationic polyelectrolyte are effectively neutralized and further addition of the cationic polyelectrolyte does not affect the swelling behaviour of the fibres.[44] The results of Swerin *et al.*[44] show efficiently the same amount of polybrene (between 1% and 3%) to achieve the maximum deswelling for a wide variety of pulps, including one similar to ours. It is worth noting that the charge stoichiometry is closely followed in the fibre–polyelectrolyte system at low ionic strength ($\sim 10^{-3}$ M) since the range of electrostatic force fields is larger than the mean distance between the charges on the fibre surface. At sufficiently high ionic strength ($>10^{-2}$ M) the charges in the hemicellulose backbone can act as point charges because the average separation of the charges is rather large, *i.e.*, ~1.6 nm according to the length and width of the xylanose ring (~0.5 nm) and the mean distance of charges in the xylan backbone (~10 xylanose units).[45] However, because of the low ionic strength, this ambiguity is avoided in our research. The final notion is for the different values of the measured pore volumes. WRV and TPM do not yield the same values because the TPM has an upper limit of pore size diameter (220 nm). This gives an opportunity to estimate the volume of different pores by comparing WRV and TPM values.

In short, three detectable types of water are present in the fibre cell wall: (i) water tightly bound to the surface of the microfibrils (*i.e.*, non-freezing water, NFW), (ii) water residing in micropores (2–220 nm diameter), and (iii) water residing in macropores (>220 nm diameter). NFW and the water in micropores are detectable with TPM whereas a WRV measurement quantifies all water, *i.e.*, all of the three types. It is due to the limitations of the melting point depression of the solute that not all of the water in the cell wall can be measured with TPM alone. Therefore, it seems likely that the polybrene influences only the micropore volume and the macropores are left intact, because WRV (Table 3) and TPM values (Table 3) decrease by the same amount and in addition, the measured NFW values are constant within error limits (Table 3 and Fig. S9†). This is an important observation since a low M_w polyelectrolyte can negate the charge of the fibres in two ways: either neutralizing the charge by penetrating the cell wall and reaching the charges or by accommodating enough positive charge on the surface so that the fibre–polyelectrolyte system (as observed from a distance) is neutralized. Our results indicate that at least the effect of low M_w, high charge density polyelectrolyte is to neutralize the charges only in the micropore region, that is, between the microfibrils inside the cell wall. We would like to note also that the polybrene, due to spatial reasons, adsorbs first on the surface and then inside the surface. We look at this aspect in more detail in the next section.

Fig. 3 shows the pore volume differences at a given pore diameter of hardwood kraft pulp fibres after adsorption steps with cationic polyelectrolytes as measured by TPM. Generally,

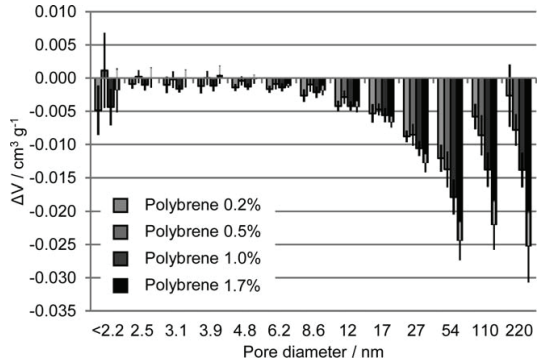

Fig. 3 Never dried samples. Pore volume difference at a given pore diameter (control reference set to zero). Polybrene has an increasing effect on the pore closure starting from ~12 nm. Fibre charge is neutralized at the 1.5% addition and, thus, a charge reversal occurs at higher loadings.

Table 3 Amounts of adsorption onto the cellulosic material as determined by polyelectrolyte titration (w/w%). Water retention values (WRVs) for the never-dried values as well as once dried samples, non-freezing water (NFW) and total bound water (TPM + NFW) for the samples as grams of water per gram of fibre. The difference of the sample compared to the control reference tabulated as ΔTPM and Δ(TPM + NFW)

			Never-dried/g per g						Dried/g per g					
	Added (%)	Ads. (%)	WRV	NFW	TPM	ΔTPM	TPM + NFW	Δ(TPM + NFW)	WRV	NFW	TPM	ΔTPM	TPM + NFW	Δ(TPM + NFW)
Reference	—	—	1.68	0.302	0.498	—	0.800	—	1.29	0.290	0.373	—	0.667	—
PDADMAC fractionated	1.00	0.17	1.65	0.313	0.451	−0.047	0.764	−0.036	1.24	0.312	0.395	0.022	0.707	0.040
PDADMAC unfractionated	1.00	0.22	1.64	0.293	0.437	−0.061	0.731	−0.069	1.22	0.298	0.376	0.003	0.673	0.006
Polybrene	0.50	0.50	1.65	0.300	0.450	−0.048	0.742	−0.058	1.19	0.292	0.391	0.018	0.685	0.018
	2.00	1.74	1.55	0.306	0.398	−0.100	0.687	−0.113	1.09	0.290	0.361	−0.012	0.650	−0.017

the pore size graphs are plotted as cumulative distributions but in this case the differences due to polyelectrolyte adsorption between various measurement points in the cumulative size distribution graphs were difficult to distinguish (Fig. S4 in the ESI†). This was the expected behaviour as the adsorbed polyelectrolytes caused only minor differences in the total water content of the cell wall (see WRV in Table 3), *i.e.*, in the order of 0.1 g per g. Therefore, to gain insight into the alterations occurring in the pore size distribution, we have set the control reference values to zero and plotted the pore volume difference to the control as a function of pore volume at a given pore diameter (Fig. 3). The control reference (no adsorption applied) correlates well with previously obtained data for other cellulosic pulp fibres.[31] The cumulative micropore volume was ~0.7 to 0.8 $cm^3 g^{-1}$ and it depends strongly on the adsorbed amount of the polybrene (Tables 3 and S2 in the ESI†). However, the cumulative pore volume with the smaller pores is decisively influenced by the amount of NFW—a measurement which is the least reliable of the whole TPM analysis.[28] Although the amounts of NFW for different samples fall within the experimental error (Table 3), minute differences in NFW can already cause drastic differences to the pores whose cumulative pore volume is on the same order of magnitude with the NFW measurement error, *i.e.*, pores with diameters ranging from 2.2 to 12 nm. We can safely say, however, that a portion of the largest pores (≥17 nm) collapse as a result of polybrene adsorption. The pore volume between 17 and 220 nm pore diameter (Fig. 3) shows that the pore volume at a given diameter is gradually reduced when the polybrene amount is increased, indicating that the cationic polyelectrolyte collapses the structure. The initial high value of 2.2 nm pores in Fig. 3 is due to the fact that <2.2 nm column contains all the pores measurable in TPM below 2.2 nm pore diameter (which equals the temperature range of −33 °C to −20 °C) resulting in an initial column with high values.

DLS measurement yielded 3 nm diameter for polybrene in 0.1 M NaCl (Table 3), but because of the higher ionic strength and the collapsed structure required by the DLS measurement the diameter is in fact larger in our low ionic strength samples. Literature values from diffusion and electrophoresis NMR indicate a hydrodynamic diameter in the order of 10 nm for a 5000 g mol^{-1} cationic polyelectrolyte in an ionic strength close to ours (1 mM $NaHCO_3$).[46] It has been estimated that the pore diameter in cellulosic fibres must be *ca.* 3–5 times larger than the hydrodynamic diameter for a polymer to fit inside a pore.[23] Accordingly, our data suggest that a polymer with 3–10 nm diameter is able to fit into pores of 9 to 50 nm diameter and subsequently collapse it by reducing the osmotic pressure. One complication which was avoided until now was the location of the adsorption. Due to our previous reasoning we can assume that polybrene reaches all the pores. However, due to spatial reasons, the surface is neutralized first. Therefore, the low adsorption amounts describe the pore changes at the surface and high adsorption amounts, inside the cell wall. Charge reversal upon the adsorption of polybrene is expected since further adsorption takes place above the neutralization point of ~1.5% (Fig. 2a). However, the charge reversal is expected to be very small due to the constraints for conformational changes induced by the small size of the polymer chain (see schematics in Fig. 4a). These conformational constraints are less prominent

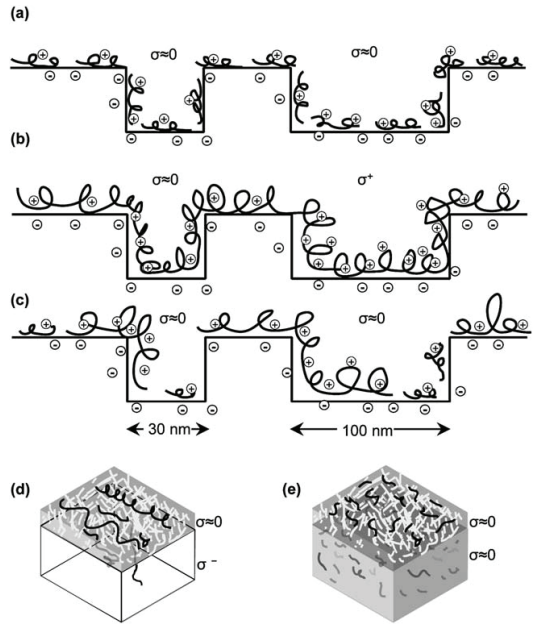

Fig. 4 Schematic representation of the polyelectrolyte adsorption into the cell wall pores of two different diameters (30 and 100 nm). The indicated pore sizes are approximate. Initially the pores are kept open by osmotic pressure caused by the negative charge. (a) Low M_w cationic polyelectrolyte adsorbs into the pores and neutralizes the cell wall polymers. This can subsequently collapse the pores due to the reduced osmotic pressure (not shown). (b) High M_w cationic polyelectrolyte adsorbs onto the surface and uncoils into the pores it can access (10–50 nm). This is bound to subsequently collapse the pores where neutralization is complete (not shown). The larger pores accommodate the high M_w polyelectrolyte fully and with a flat conformation thus inducing charge overcompensation. Subsequently the pores are kept open by the osmotic effect caused by the counter-ions of the surplus positive charge. (c) The unfractionated PDADMAC has an effect composite of that in (a) and (b). (d) The situation where the modest amount of charge is adsorbed (≤0.5%) the polyelectrolytes are mostly confined to the surfaces regardless of M_w. (e) For high amounts of charge (>0.5%) the polymers can penetrate into the cell wall. This is bound to subsequently cause the pores to collapse (not shown).

in longer polymer chains and their explicit impact resulting in higher charge reversal has been explored in the following section.

The effect of surface adsorbing polymers on the whole pore size distribution. By selectively choosing a polymer that cannot adsorb inside the cell wall, we can gain information regarding the porosity changes on the surface as well as inside the cell wall. We chose high M_w PDADMAC as the surface adsorbing polymer since it has long been indirectly assumed[1] and recently verified[2] that high M_w PDADMAC adsorbs exclusively on the surface of cellulosic fibres. Our own data concur with this information because the adsorbed amounts of PDADMAC and polybrene were substantially different (Fig. 2a and S2†). Since the low M_w part of the PDADMAC M_w-distribution might interfere with the

results we also employed fractionated PDADMAC—where the low M_w fraction had been removed—to see if the low M_w fraction has an impact on the pore size distribution. The adsorption isotherms of fractionated and unfractionated polymers also revealed that there is a substantial amount of low M_w fraction adsorbed inside the cell wall, since the adsorbed amounts differ by 100% at a PDADMAC equilibrium concentration of 100 mg dm^{-3} (Fig. S2†). Fig. 5 demonstrates the effect of the fractionated and unfractionated PDADMAC on the surface pores. Here, we have again set the control reference values to zero and plotted the pore volume difference to the control reference as a function of pore volume at a given pore diameter. In addition, the pore size distribution after 0.5% polybrene addition has been plotted to compare the effect of M_w on the pore size distribution. We chose the 0.5% addition, since the adsorbed amount of charge was roughly similar when we take the charge density of the polymers into account (Table 2). In addition, lower dosages such as 0.5% should neutralize mainly the fibre surface because of spatial constraints as described in the previous passage. Fig. 5 exhibits similar adsorption effects for similar charge for unfractionated PDADMAC and polybrene, although the unfractionated PDADMAC appears to induce a slightly more pronounced decrease in the pore volumes than polybrene does. On the other hand, even though possessing a similar effect in the range of 9–50 nm pore diameter region, the sample treated with fractionated PDADMAC appeared to have lower pore volumes for <2.2 nm diameter pores than the control reference or the samples treated with other polyelectrolytes. Conversely, with the largest pore size diameters (110–220 nm) the pore volume stayed intact or even increased slightly after adsorption of fractionated PDADMAC. Previously, we argued that polybrene could access the pores in the range of 9 to 54 nm. Unexpectedly, the adsorption of both fractionated and unfractionated PDADMAC appeared to cause pore closure in this region (Fig. 5). We can hypothetically argue this apparent similarity arising from the coiled (3D) conformation of the PDADMAC in the solution and a flat extended (2D) coil conformation in the adsorbed state.[47,48] The 3-dimensional coiled polymer undergoes rapid adsorption and rearrangement to a flat conformation on the surface, which enables it to access all the charges inside the pores it has freedom to access (Fig. 4b). This takes place mainly on a thin outer surface layer, as elucidated by the confocal microscope images of Horvath *et al.*[2] The accessibility of the surface pores upon reconformation would then explain why the pore collapse of polybrene 0.5% and both the PDADMACs has similar effects in the 9–54 nm pore diameters (Fig. 4a and b).

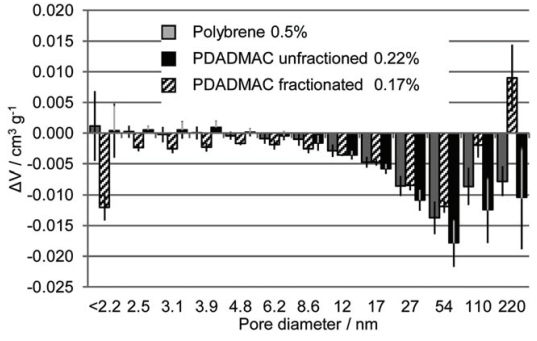

Fig. 5 Never-dried samples with similar amounts of positive charge adsorbed onto the fibres. We attribute the changes in the figure to polymers that have been adsorbed mainly onto the surface, according to Horvath *et al.*[2] Pore volume difference at a given pore diameter (control reference set to zero). The results for fractionated and unfractionated PDADMACs, and polybrene 0.5% are shown as a comparison.

In contrast to the smaller pores, the behaviour of the pores in the 110 to 220 nm region is clearly distinct for each sample (Fig. 5). We argue that the increase in the size of the larger pores after the adsorption of fractionated PDADMAC (Fig. 5) can be hypothetically attributed to the charge reversal and the overcompensation of positive charge—*i.e.*, increased osmotic pressure—on the porous fibre surface where the largest pores reside (Fig. 4b). This speculative effect of overcompensation is not that substantial for polybrene because the overcompensation with PDADMAC is bound to be greater than with polybrene due to the larger degree of freedom of the polymer backbone to move and change the conformation. This can be seen clearly, for example, in a more rapid thickness increase of multilayer films with high M_w PDADMAC in contrast to a lower M_w polyelectrolyte.[48] Since this phenomenon is absent from the adsorption of unfractionated PDADMAC we argue—based also on the SEC data (Fig. S1†)—that the low M_w part of the distribution once adsorbed into the large pores (110 to 220 nm diameter) sufficiently decreases the surplus charge in order to negate the overcompensation effect (Fig. 4c). The second prominent difference between the influence of fractionated PDADMAC and the other polymers on the pore volume is visible within the smallest pores from 2.2 to 3.9 nm diameter (Fig. 5). They have less pore volume after fractionated PDADMAC adsorption than the control reference and the other polymer samples. This cannot be fully explained by the experimental error in NFW and in the first 2.2 nm pore region. We would like to consider one possible explanation for these results. A polymer can move inside a porous structure by random wiggling, called reptation, given that the polymer fulfils certain criteria, even if the pore is smaller than the hydrodynamic diameter. Mishael and his coworkers found that high ionic strength and longer adsorption time facilitate reptation inside controlled pore glasses (CPGs).[4] In our case, however, the ionic strength is much lower which decelerates reptation. The pores are negatively charged, unlike the non-charged pores in CPG, so that there is an extra contribution to the free energy for reptation when the pores are neutralized by the cationic polyelectrolyte inside the cell wall. To conclude, it is hard to distinguish if the initial values for the fractionated PDADMAC would be an experimental error or an indication of a reptation inside the porous structure. The hypothetical reptation is hindered with the unfractionated PDADMAC, because the low M_w fraction can access the negative charges inside the cell wall thus negating the free energy contribution for the unfractionated PDADMAC. As a final note, the effects in the porous structure in the surface can be assigned only to micropores (<220 nm diameter pores), since the WRV of the fibres after the adsorption of the polymers (Table 3) underwent a minute decrease (from 1.68 to 1.65 or 1.64) which is quantitatively similar to the values measured by TPM (from 0.800 to 0.764 or 0.731).

Adsorption *vs.* porosity with dried fibres

When cellulosic fibres are dried, water is removed from between the cellulose microfibrils and the fibre structure becomes essentially non-porous.[49] The porosity is regained by eventually re-exposing the fibre to water. With chemical pulp fibres, however, a large portion of the pores have closed irreversibly upon drying. This phenomenon, dubbed hornification, has received a lot of coverage in the literature and its diminishing effect on pore size distribution has been explicitly elaborated.[50–52] From the fundamental point of view, the influence of adsorbed polyelectrolytes on the irreversible pore closure upon drying is an interesting concept. It enables the differentiation between the effects of the physical act of drying and the physicochemical act of polyelectrolyte adsorption. Drying has minimal changes in chemical and physical properties apart from the pore size distribution. Many studies have been conducted to see the effect of drying for chemical pulp fibres, and the conclusion seems to be that there are no detectable changes in crystallinity and chemical composition upon drying.[53] The drying induces capillary forces to the microfibrillar structure and closes all pores in a definite order.[49,54] Rewetting the samples opens only those pores which are accessible to water. The sum of these effects can be seen in the difference of WRV (Table 3) which describes the accessibility of water to the cell wall. The differences between the dried and never-dried samples are quite substantial (~0.40 to 0.50 g per g), and they are much larger than the adsorbed polyelectrolyte effect for the never-dried fibres (~0.05 g per g for low adsorption and ~0.15 g per g for high adsorption amounts). This is due to capillary forces during drying. It is an additional force acting on the fibrils and forcing them to irreversibly close more strongly than with a decrease in osmotic pressure alone. The micropore effect of drying for control reference is shown in Fig. 6a. Here, the actual pore volume distribution of the control reference (untreated, never-dried fibres) has been expressed in white columns whereas the negative values, denoted by the black columns, correspond to the decrease in pore volume after drying and rewetting the fibres. There is a slight decrease in the <2.2 nm diameter pores and a substantial decrease starting from ~17 nm diameter pores. This measurement directly indicates that the pores with diameters 2.5–17 nm are scarcely affected by drying. This might be an important item in the discussion of the porosity of the cellulosic fibres in the wet state. The cumulative pore volumes of the once dried samples exhibit smaller values than the never-dried samples starting from ~17 nm and the effect is most pronounced for the large pores (110–220 nm). These results correlate also with the microscopic treatise of Duchesne and Daniel[55] and TPM by Wang *et al.*[56] The error of the method is larger for the dried samples compared to the never-dried samples due to the additional forces, such as the capillary force, acting on the structure in the drying process. Therefore, the cumulative pore volumes of the samples appear to have similar pore size distributions (Fig. S6 and S7 in the ESI†). To gain additional insight into the effect of polyelectrolyte adsorption on drying, we have plotted the actual pore volume differences with respect to the control reference for dried fibres at a given diameter (Fig. 6b). We emphasize that the polyelectrolytes have been adsorbed on the fibres prior to drying to illuminate the influence of polyelectrolytes on the irreversible pore closure. A wide variation exists within the smallest pore diameters (<2.2 nm) while almost no changes were seen in comparison to the dried control reference in the region 2.5–17 nm, and even at 27 nm the changes in the osmotic pressure induced by polyelectrolyte adsorption appear to play a minimal role in the pore volume (Fig. 6b). We speculated in the previous section that for the fractionated high M_w PDADMAC the overcompensation would keep the pores open upon adsorption, while the low M_w polybrene, lacking this charge reversal, should not have this pore retaining capability. These hypotheses appear valid also when interpreting the polyelectrolyte effect on the pore closure upon drying. Complete neutralization by polybrene adsorption (2.0%) facilitates the irreversible pore closure with larger pore diameters because of the lack of charge repulsion inside the pore (Fig. 6b). The hypothetical overcompensation in the larger pores by fractionated PDADMAC helps reopen these larger pores after drying (Fig. 6b). Both the unfractionated PDADMAC and polybrene (0.5% addition) had an effect that was a combination of the effects of the fractionated PDADMAC and polybrene (2.0%) and they seem to have no effect on the pore size distribution of the dried substrates apart from the small difference in the <2.2 nm pores. The hypothetical reptation of the fractionated PDADMAC molecules can be seen in the small pores in the region of 2.5–12 nm, but this might well be an experimental error.

It is clear from the TPM results and their interpretation (Fig. 3–6) that pore size distribution of water-swollen cellulosic fibres can be selectively tuned with polyelectrolyte adsorption.

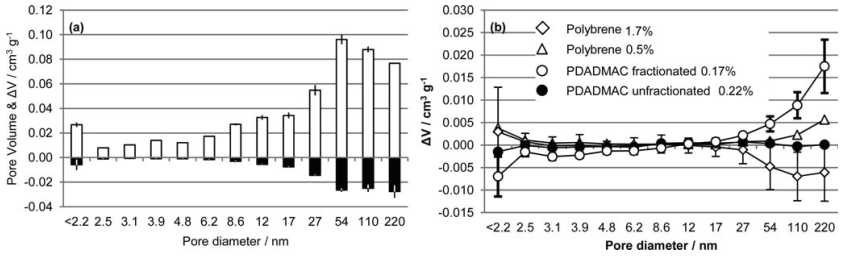

Fig. 6 The effect of drying. (a) The pore volume of the never-dried control reference (white columns) and the changes in the pore volume after drying and rewetting (black columns). (b) The effect of drying on pore size distribution of the polyelectrolyte treated fibres (control reference for dried fibres is set to zero). Note the scale difference in the ordinates between (a) and (b). The error bars for polybrene 0.5% and PDADMAC unfractionated 0.22% have been omitted for clarity (see Fig. S8† for all the error bars.).

Distinct effects on pores of particular diameter were observed with different molecular weights (high *vs.* low M_w) and molecular weight distributions (fractionated *vs.* unfractionated polyelectrolyte). It is possible that further simple parameters, such as charge density of the polyelectrolyte or electrolyte concentration of the solution, can be applied to tune the pore size distribution in an even more precise fashion. Although cellulosic fibres are special materials, many hydrogels possess polyelectrolyte character and their pore size should be susceptible to alterations by polyelectrolyte adsorption. Moreover, the pore size distributions of hydrogels are not usually retained after simple drying.[57] As the pore size of hydrogels is important in many of their applications, from tissue engineering[58] to wound dressing,[59] a conceptual approach for the adjustment of the pore size distribution represents an interesting idea for materials scientists working with water-swollen materials.

Conclusions

In this work, we have investigated the effect of polyelectrolyte adsorption on the pore size distribution of cellulosic (chemical wood pulp) fibres. We have demonstrated the decrease of micropore volume for cationic polyelectrolytes as well as the effect of low and high M_w fractions to this decrease. Cationic polyelectrolytes neutralize the charges and thus induce an osmotic pressure driven collapse in the pores where the electrostatic repulsion is gone, in some cases the charge reversal can be attributed to the small pore volume retaining effect. The size of the polyelectrolyte determines which pores are reached by the polyelectrolyte and thus what regions are charge-neutralized. The combined effect of physical action (drying) and physicochemical treatment (polyelectrolyte adsorption) was also examined. After drying the polyelectrolyte treated fibres, the pore size distribution is altered with a notable lack of effect in the 2.5–17 nm pore diameters. The effect of the polyelectrolytes after drying was visible although in a suppressed form. Although the results are not universally applicable for all hydrogels, the study presents a concept of fine-tuning the pore size distribution for water-swollen materials that possess a polyelectrolyte character.

Acknowledgements

The assistance of Leena Nolvi with the thermoporosimetry measurements is kindly acknowledged. SEC measurements of the cationic polyelectrolytes by Jukka Rautiainen and Kemira Oyj are acknowledged. Financing from the ChAD project—Botnia, Kemira, UPM, Andritz and Finnish Centre for Technology and Innovation (TEKES)—is greatly acknowledged.

References

1 L. Wågberg, L. Ödberg and G. Glad-Nordmark, *Nord. Pulp Pap. Res. J.*, 1989, **4**, 71.
2 A. T. Horvath, A. E. Horvath, T. Lindström and L. Wågberg, *Langmuir*, 2008, **24**, 7857–7866.
3 A. T. Horvath, A. E. Horvath, T. Lindström and L. Wågberg, *Langmuir*, 2008, **24**, 6585–6594.
4 Y. G. Mishael, P. L. Dubin, R. de Vries and A. B. Kayitmazer, *Langmuir*, 2007, **23**, 2510.
5 A. M. Scallan, *Tappi J.*, 1983, **66**, 73–75.
6 T. Tammelin, T. Saarinen, M. Österberg and J. Laine, *Cellulose*, 2006, **13**, 519–535.
7 G. V. Laivins and A. M. Scallan, *J. Pulp Pap. Sci.*, 1996, **22**, J178–J184.
8 P. Zugenmaier, *Crystalline Cellulose and Cellulose Derivatives: Characterization and Structures*, Springer-Verlag GmbH, Berlin, 2008.
9 C. Laine, W. Xinshu, M. Tenkanen and A. Varhimo, *Holzforschung*, 2004, **58**, 233–240.
10 A. J. Panshin and C. De Zeeuw, *Textbook of Wood Technology*, McGrawHill Inc., USA, 1970, p. 91.
11 B. Alince, *Nord. Pulp Pap. Res. J.*, 2002, **17**, 71–73.
12 A. Kongdee, T. Bechtold, E. Burtscher and M. Scheinecker, *Carbohydr. Polym.*, 2004, **57**, 39.
13 N. Wu, M. A. Hubbe, O. J. Rojas and S. Park, *BioResources*, 2009, **4**, 1222–1262.
14 H. Tanaka, K. Tachiki and M. Sumimoto, *Tappi*, 1979, **62**, 41–44.
15 L. Wågberg, *Nord. Pulp Pap. Res. J.*, 2000, **15**, 586–597.
16 L. Wågberg and R. Hägglund, *Langmuir*, 2001, **17**, 1096–1103.
17 C. Cheng, A. W. Martinez, J. Gong, C. R. Mace, S. T. Phillips, E. Carrilho, K. A. Mirica and G. M. Whitesides, *Angew. Chem., Int. Ed.*, 2010, **49**, 4771–4774.
18 J. L. Delaney, C. F. Hogan, J. Tian and W. Shen, *Anal. Chem.*, 2011, **83**, 1300–1306.
19 L. Ye, C. D. M. Filipe, M. Kavoosi, C. A. Haynes, R. Pelton and M. A. Brook, *J. Mater. Chem.*, 2009, **19**, 2189–2198.
20 R. T. Olsson, M. A. S. Azizi Samir, G. Salazar-Alvarez, L. Belova, V. Strom, L. A. Berglund, O. Ikkala, J. Nogues and U. W. Gedde, *Nat. Nanotechnol.*, 2010, **5**, 584–588.
21 P. J. Bracher, M. Gupta and G. M. Whitesides, *Soft Matter*, 2010, **6**, 4303–4309.
22 L. Salmén and J. Berthold, *Fundam. Papermaking Mater., Trans. Fundam. Res. Symp., 11th*, 1997, **2**, 683–701.
23 B. Alince and T. G. M. Van de Ven, *Fundam. Papermaking Mater., Trans. Fundam. Res. Symp., 11th*, 1997, **2**, 771–788.
24 M. Häggkvist, D. Solberg and L. Wågberg, *Nord. Pulp Pap. Res. J.*, 1998, **13**, 292–298.
25 T. G. M. van de Ven, *Nord. Pulp Pap. Res. J.*, 2000, **15**, 494–500.
26 M. Iza, S. Woerly, C. Danumah, S. Kaliaguine and M. Bousmina, *Polymer*, 2000, **41**, 5885–5893.
27 T. Maloney, *Pre-Symp. ISWPC, 10th, Recent Adv. Pap. Sci. Technol.*, 1999, vol. 1, p. 245.
28 T. Maloney, J. E. Laine and H. Paulapuro, *Tappi J.*, 1999, **82**, 125–127.
29 S. Park, R. A. Venditti, H. Jameel and J. J. Pawlak, *Cellulose*, 2006, **13**, 23–30.
30 S. Park, R. A. Venditti, H. Jameel and J. J. Pawlak, *Carbohydr. Polym.*, 2006, **66**, 97.
31 T. C. Maloney and H. Paulapuro, *Sci. Papermaking, Trans. Fundam. Res. Symp., 12th*, 2001, vol. 2, pp. 897–926.
32 D. da Silva Perez and A. R. P. van Heiningen, *7th EWLP Proc.*, 2002, vol. 1, pp. 393–396.
33 S. Rovio, H. Simolin, K. Koljonen and H. Sirén, *J. Chromatogr., A*, 2008, **1185**, 139–144.
34 A. Swerin and L. Wågberg, *Nord. Pulp Pap. Res. J.*, 1994, **9**, 18.
35 L. Wågberg and L. Odberg, *Nord. Pulp Pap. Res. J.*, 1989, **2**, 135–140.
36 N. K. Bhardwaj, T. D. Duong and K. L. Nguyen, *Colloids Surf., A*, 2004, **236**, 39–44.
37 K. Ishikiriyama and M. Todoki, *J. Colloid Interface Sci.*, 1995, **171**, 103–111.
38 T. C. Maloney, H. Paulapuro and P. Stenius, *Nord. Pulp Pap. Res. J.*, 1998, **13**, 31–36.
39 A. Teleman, V. Harjunpää, M. Tenkanen, J. Buchert, T. Hausalo, T. Drakenberg and T. Vuorinen, *Carbohydr. Res.*, 1995, **272**, 55.
40 J. Fahlén and L. Salmén, *Biomacromolecules*, 2005, **6**, 433–438.
41 J. Grignon and A. M. Scallan, *J. Appl. Polym. Sci.*, 1980, **25**, 2829–2843.
42 A. M. Scallan and J. Grignon, *Sven. Papperstidn.*, 1979, **82**, 40–47.
43 A. M. Scallan and J. E. Carles, *Sven. Papperstidn.*, 1972, **75**, 699–703.
44 A. Swerin, L. Ödberg and T. Lindström, *Nord. Pulp Pap. Res. J.*, 1990, **5**, 188.
45 A. E. Horvath, T. Lindström and J. Laine, *Langmuir*, 2006, **22**, 824.
46 U. Böhme and U. Scheler, *J. Phys. Chem. B*, 2007, **111**, 8348–8350.
47 M. Österberg, *J. Colloid Interface Sci.*, 2000, **229**, 620–627.
48 L. Wågberg, G. Decher, M. Norgren, T. Lindström, M. Ankerfors and K. Axnäs, *Langmuir*, 2008, **24**, 784–795.

49 J. E. Stone, A. M. Scallan and G. M. A. Aberson, *Pulp Pap. Mag. Can.*, 1966, **67**, T263.
50 G. V. Laivins and A. M. Scallan, *Prod. Papermaking., Trans. Fundam. Res. Symp., 10th*, 1993, vol. 2, pp. 1235–1260.
51 M. A. Hubbe, R. A. Venditti and O. J. Rojas, *BioResources*, 2007, **2**, 739–788.
52 U. Weise, *Pap. Puu*, 1998, **80**, 110–115.
53 K. L. Kato and R. E. Cameron, *Cellulose*, 1999, **6**, 23.
54 D. Topgaard and O. Söderman, *Cellulose*, 2002, **9**, 139.
55 I. Duchesne and G. Daniel, *Nord. Pulp Pap. Res. J.*, 1999, **14**, 129–139.
56 X. Wang, T. C. Maloney and H. Paulapuro, *Appita J.*, 2003, **56**, 455–459.
57 J. Weber and L. Bergström, *Macromolecules*, 2009, **42**, 8234–8240; J. Weber and L. Bergström, *Langmuir*, 2010, **26**, 10158–10164.
58 F. A. Landis, J. S. Stephens, J. A. Cooper, M. T. Cicerone and S. Lin-Gibson, *Biomacromolecules*, 2006, **7**, 1751–1757.
59 F. Yanez, J. L. Gomez-Amoza, B. Magariños, A. Concheiro and C. Alvarez-Lorenzo, *J. Membr. Sci.*, 2010, **365**, 248–255.

Electronic Supplementary Information

for

Influence of adsorbed polyelectrolytes on pore size distribution of a water-swollen biomaterial

Niko Aarne, Eero Kontturi,* Janne Laine
Department of Forest Products Technology, School of Chemical Technology, Aalto University, P.O.Box 16300, 00076 Aalto, Finland
*) Corresponding author. Email: eero.kontturi@aalto.fi; Phone: +358 945124250; Fax: +358 945124259.

Electronic supplementary information includes Size exclusion chromatography (SEC) data for the cationic polymers used (S1), calculation of the effect cryoscopic effect of the salt (S2), adsorption isotherms for poly(diallyl dimethyl ammonium chloride) (PDADMAC) samples (S3) and the differential scanning calorimeter (DSC) data as the cumulative pore volume with error limits and the DSC data converted to volume and pore diameter size. (S4)

S1 Size exclusion chromatography data for the cationic polymers used

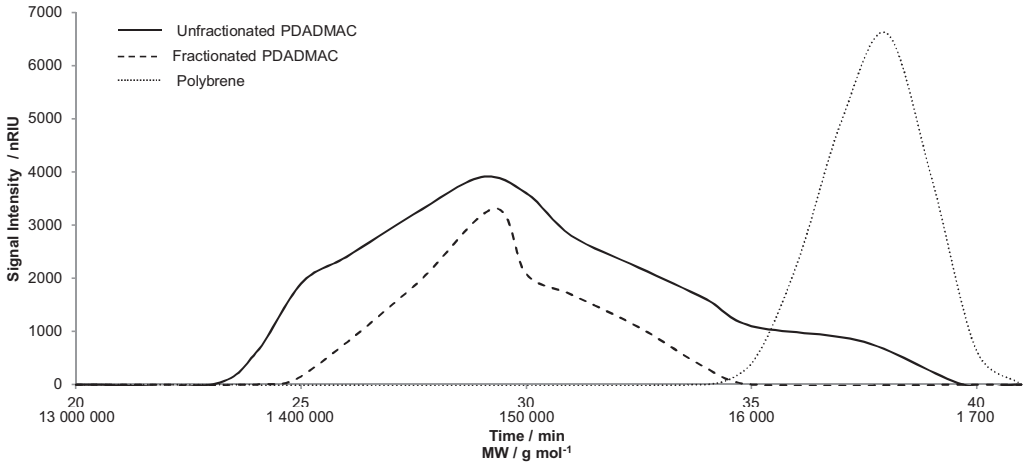

Figure S1. The SEC data for the cationic polymers used. The fractionated PDADMAC and polybrene had no overlap while the unfractionated PDADMAC had a part of the distribution in the polybrene MW range.

S2 Calculation of the cryoscopic effect of the salt

This calculation intends to show that the cryoscopic effect of the salt is minimal to our samples and does not affect the samples during DSC analysis. The cryoscopic effect (freezing-point depression) can be calculated from the well-known equation:

$$\Delta T_F = K_F \cdot b \cdot i, \qquad \text{(S1)}$$

where ΔT_F is the freezing point depression, K_F the cryoscopic constant (for water ~1.9 K·kg/mol), b the molality of the solvent, i is the van't Hoff factor (in our case just 2 since we assume simple monovalent ions to be dissolved *i.e.* NaCl.) Our samples (fibres dispersed in water) exhibited conductivity of <5 µS/cm before analysis (typical value was 3.2 µS/cm). From a tabulated reference we obtain conductivity of roughly 10^{-4} molality.[S1] Several other methods can be used: For NaCl, either by solving the concentration using Kohlrausch's law:

$$\kappa = \Lambda^0_m \cdot c - K \cdot c^{1.5}, \qquad \text{(S2)}$$

where κ is the conductivity, Λ^0_m the limiting molar conductivity, c the concentration and K Kohlrausch constant) with 126.5 S cm^2/mol as limiting molar conductivity (of NaCl) and *ca.* -2100 S·cm$^{3.5}$·mol$^{-1.5}$ as the Kohlrausch constant (for water-NaCl system) or simply by measuring the conductivity of a series of NaCl solutions (10^{-3}-10^{-5} M) and comparing the sample conductivity with the series. With this we obtain molarity between 10^{-4}-10^{-5} M and thus maximum molality of ~10^{-4} mol/kg. Using these values in equation (S1) yields a freezing point depression of ~0.00038 K (1.9 K·kg/mol·10^{-4} mol/kg·2 K), a value small enough to consider its influence insignificant.

S3 Adsorption isotherms for unfractionated and fractionated PDADMAC samples

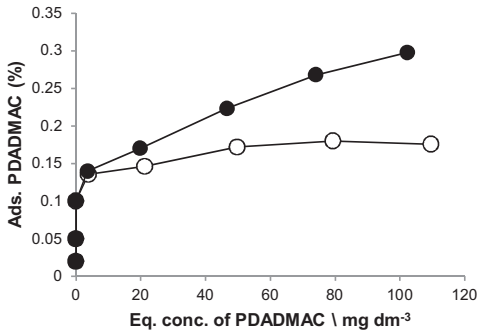

Figure S2. Adsorption isotherms for unfractionated (●) and fractionated (○) PDADMAC samples. The adsorbed amounts were weight-percentage per unit mass of fibre. Equilibrium concentration was the unadsorbed PDADMAC in the solution after 30 mins. Ionic strength was 1 mM ($NaHCO_3$) and pH ~9. The fractionated sample had a constant adsorption of about 0.15% while the unfractionated sample had increasing adsorption due to the adsorption of the low molecular weight (MW) part of the MW distribution of the unfractionated PDADMAC.

S4 Cumulative pore volume data with error limits and the pore size distribution data from the DSC measurements.

We have added the actual data from the DSC measurements to exemplify the measurement details (Figure S3). The cumulative pore size distribution is the most common way to describe the pore size distribution obtained from differential scanning calorimeter (DSC) data with step-melting (Figure S4-6) and is therefore added here as a reference. The basis for this work was laid in the fundamental efforts of Maloney to employ DSC to study the pore size diameters found in the wet-state of the cellulosic fibres. For the equations and a method how to convert the DSC data to pore size distribution, see the main article and the references therein. The measurement error in cumulative pore size distribution is composed of the cumulative error of 13 independent measurements which have been added together. This produces error that is much larger than each individual measurement alone. In addition, the difficulties in homogenising the samples, *i.e.,* when the fibres are treated with less than equilibrium adsorption some fibres may obtain more and some less than the optimal amounts. In these cases the measurements were increased to obtain better results.

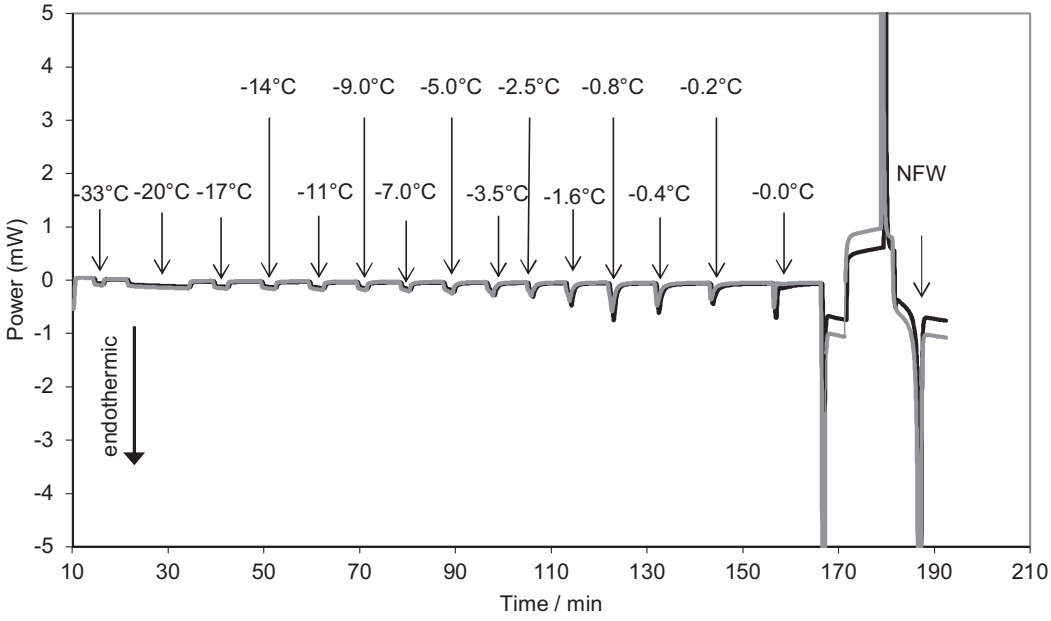

Figure S3. Example data from DSC measurement for illustrative purpose. The graph indicates the endothermic melting at different times. The indicated temperatures correspond to the isothermal steps. The non-freezing water (NFW) is calculated from the melted and refrozen sample and the peak is shown in the figure on the right. Grey line is for the control reference and black line for fibres adsorbed with 2.0% of polybrene.

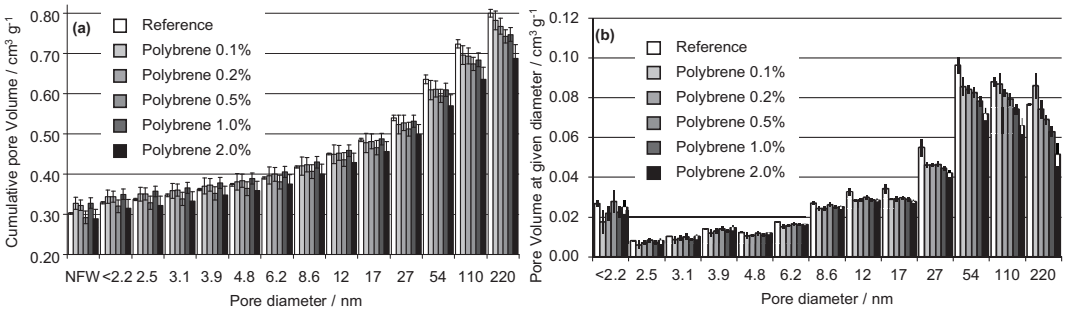

Figure S4. (a) Cumulative pore size distributions for never-dried fibre samples adsorbed with indicated amounts of polybrene (weight percentage). (b) The pore size distributions for the same samples as in (a).

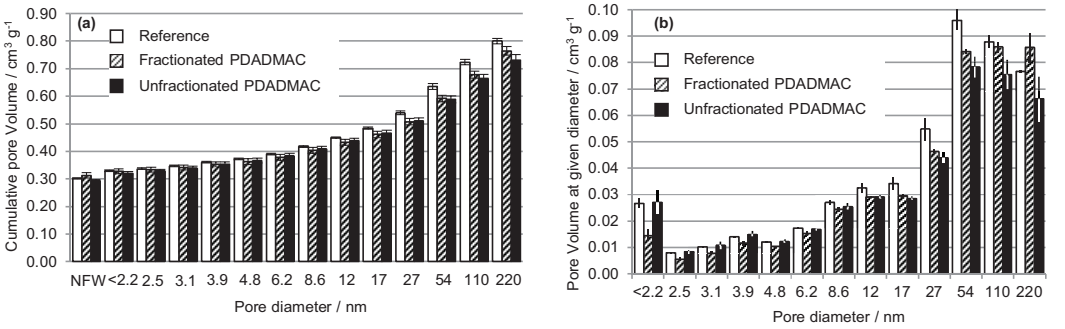

Figure S5. (a) Cumulative pore size distributions for never-dried fibre samples adsorbed with PDADMACs of different origin. (b) The pore size distributions for the same samples as in (a).

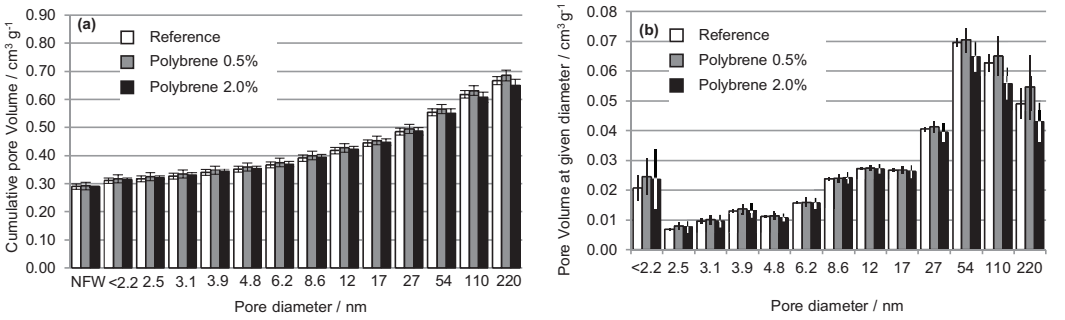

Figure S6. (a) Cumulative pore size distributions for dried fibre samples adsorbed with indicated amounts of polybrene (weight percentage). (b) The pore size distributions for the same samples as in (a).

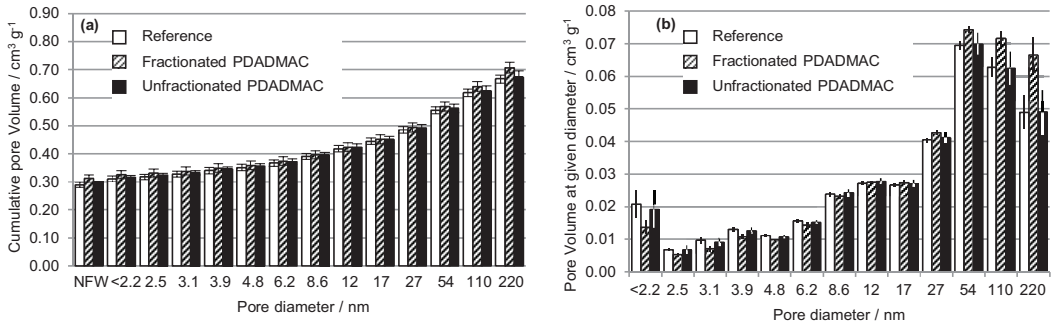

Figure S7. Cumulative pore size distributions for dried fibre samples adsorbed with PDADMACs of different origin. (b) The pore size distributions for the same samples as in (a).

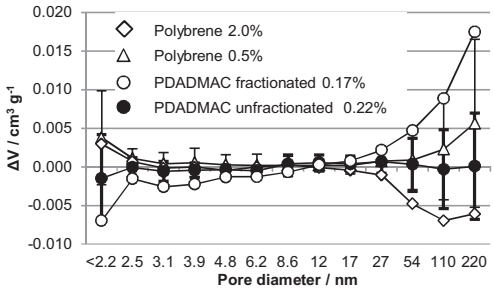

Figure S8. The effect of drying on pore size distribution of the polyelectrolyte treated fibres (control reference for dried fibres is set to zero). Error bars for the samples polybrene 0.5% and unfractionated PDADMAC 0.22%.

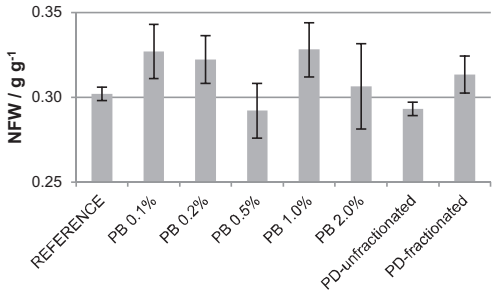

Figure S9. The non-freezing water (NFW) with error limits for all never-dried samples. Average NFW was 0.307±0.015 mL/g.

References:

[S1] R. B. McCleskey, *J. Chem. Eng. Data*, 2011, **56**, 317–327